PERFORMANCE TESTING OF ADVANCED LEAD–ACID BATTERIES FOR ELECTRIC VEHICLES

B. K. MAHATO, G. H. BRILMYER and K. R. BULLOCK

Corporate Applied Research, Johnson Controls, Inc., P.O. Box 591, Milwaukee, WI 53201 (U.S.A.)

(Received May 24, 1985; in revised form July 22, 1985)

Summary

New applications for lead–acid batteries, such as electric vehicle propulsion, demand high specific energy and power and good cycle life. A research and development program at Johnson Controls, Inc., sponsored in part by the United States Department of Energy through Argonne National Laboratory, has been underway since 1978 to develop advanced electric vehicle batteries. Cell test results on an advanced battery design developed under this program are described. Capacity, energy and power delivered at various discharge rates are shown. The effects of discharge rate and temperature on the material utilization of both electrodes are determined. The discharge capacities and charging characteristics during cycle life testing to 100% depth of discharge are also presented.

Introduction

The program established by the United States Department of Energy through Argonne National Laboratory for development of lead–acid batteries for electric vehicles consisted of two phases. The first phase was a 3-year effort to develop an improved state-of-the-art (ISOA) electric vehicle battery. The perfomance of two sizes of ISOA batteries developed by Johnson Controls, Inc., the EV2300 and the EV3000, is described elsewhere [1].

In the second phase of the program, the goals shown in Table 1 for an advanced lead–acid battery were established [2]. This paper describes the performance of one advanced battery developed by Johnson Controls, Inc., which was designed to meet the 1983 goals.

Developing the ISOA and advanced batteries was a cooperative effort of many people in both the Battery Engineering and Corporate Applied Research Groups of Johnson Controls, Inc. The batteries were designed and their performance predicted using a comprehensive proprietary model of the lead–acid system developed by Tiedemann and Newman [3, 4]. A cell

Elsevier Sequoia/Printed in The Netherlands

TABLE 1

U.S. Department of Energy goals for the advanced lead–acid battery

	1983	1986
Specific energy (3-hr rate to 1.75 V per cell)	45 W h/kg	56 W h/kg
Vol. energy density	100 W h/l	120 W h/l
Specific power (30 s av. at 50% DOD to 1.4 V per cell)	104 W/kg	104 W/kg
Energy efficiency	>75%	>75%
Life (at 80% DOD)	650 cycles	800 cycles

testing and computer-controlled data acquisition system was designed early in the program to allow rigorous testing of prototype cells [5]. Fundamental studies of the effects of impurities [6], additives [7, 8], design and application parameters were an integral part of the effort. Because the external environment, maintenance and electrical control of the battery, as well as its design, are crucial to good performance and cycle life, subsystems for charging, watering and thermal management were also developed [2, 9 - 16].

Experimental method

The advanced battery described here is the same size as the EV3000 ISOA battery, 38.1 cm long, 33.0 cm wide, and 29.5 cm high, including the manifolds and posts. The weight of the advanced design is 75.0 kg for a 12 V module with the acid circulation subsystem included, compared with 73.1 kg for the EV3000. The advanced design incorporates all the features of the ISOA battery, which are summarized in Table 2 [1]. The major change in the advanced design from the ISOA EV3000 design is the use of 15 rather than 11 electrodes per cell. The advanced design gives increased material utilization by increasing the surface area and decreasing plate thickness.

TABLE 2

ISOA and advanced battery design features

1. Thin-walled polypropylene case [19]
2. Low-resistance intracell welds [18]
3. Glass mat and microporous polyethylene envelope separator [9]
4. Radial grid design [9, 10, 17]
5. Electrolyte circulation system [2, 9 - 15]
6. Semiautomatic venting and watering subsystem [2]
7. Thermal management system [2, 9 - 15]
8. Programmable charger for overcharge control [15]

The tests described here were run on single cells equipped with an acid circulation subsystem and $Hg/Hg_2SO_4/5.7$ M H_2SO_4 reference electrode. The cyclers and data acquisition system, which have previously been described [5], were designed to monitor cell voltages and currents, half-cell potentials, charge and discharge times and temperature. Capacities and energies were calculated automatically.

Cells were discharged at constant current to 1.75 V (100% depth of discharge). Two cycles were run per day. Recharge was at a constant current of 48 A to a voltage limit of 2.5 - 2.65 V. Overcharge was controlled at 3 - 8%.

Data on the effect of discharge rate on the cell capacity were obtained from three cells which were first cycled using a constant-current, 83 A discharge to 1.75 V for 20 to 38 cycles until their capacities were well established. At this rate the capacities of the three cells were nearly identical. The cells were subsequently discharged at the 3-, 4.5- and 9-hour rates.

Studies on the effect of temperature on the capacity and material utilization of standard positive and negative plates were carried out on three plate cells. Cells with one positive and two negative plates were tested to determine the positive material utilization, whereas cells with one negative and two positive plates were tested to determine the negative material utilization. The cell temperature, which was controlled to within 1 °F, was monitored during discharge. Recharge of the cells discharged at low temperature was done at room temperature.

Failure modes of cycled cells were determined by (1) analyzing their electrochemical characteristics and (2) examining the quality of the positive and negative active materials. The positive active material was fractionated into shed, softened and retained material. The shed material was collected from the bottom of the cell. The material left on the plates was rinsed with water to separate the softened material from that retained on the grid after the rinse. Plate materials were analyzed for lead, lead dioxide, lead sulfate and antimony by wet methods. Surface areas were determined by BET.

Results and discussion

Peukert plots for the advanced battery and the EV3000 are shown in Fig. 1. According to Peukert's empirical equation [20],

$$\log t = \log C - n \log i$$

where t is the discharge time in hours, i is the discharge current in amps and n and C are constants which are characteristic of the battery design. Therefore, for a constant-current discharge, a log–log plot of the discharge time *versus* discharge current is a straight line of slope $-n$ and intercept log C. Values of n and log C of 1.20 and 2.83, respectively, for the advanced cell design were determined with a least squares fit of the straight line. The correlation coefficient was 0.988. These values compare with n and log C values of 1.28 and 2.91, respectively, for the EV3000 [1].

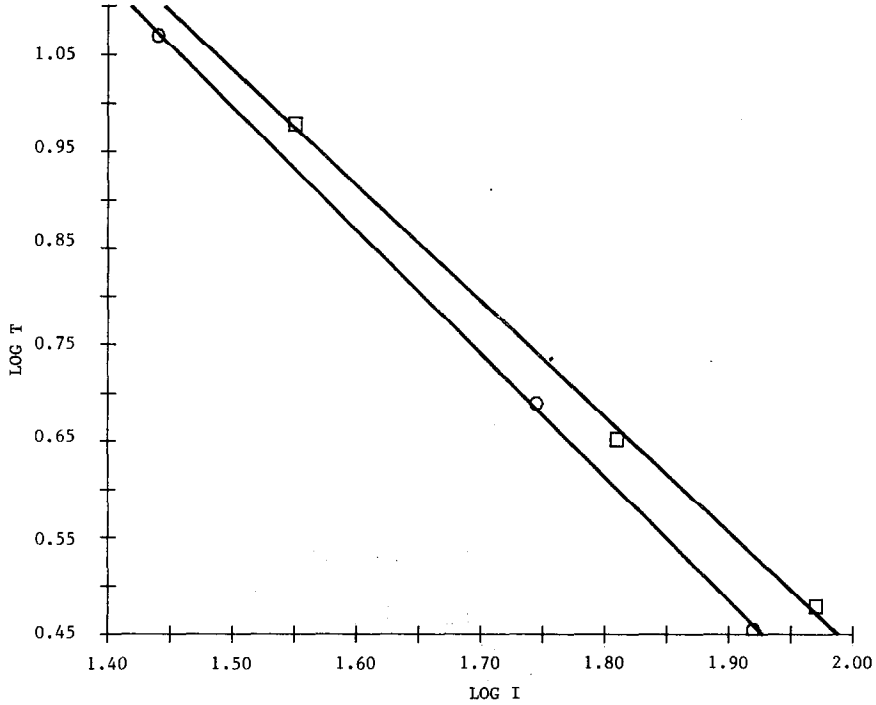

Fig. 1. Peukert plots of EV3000 (circles) and advanced (squares) cells discharged at room temperature.

The advanced cell design has a higher capacity at all currents tested. The capacity difference between the EV3000 and the advanced designs increases as the discharge current increases, as indicated by the lower *n*-value for the advanced design. Since the advanced cell has thinner plates and higher surface area, its high rate performance is better. The 1983 goal of 104 W/kg for specific power was exceeded by the EV3000 design, which has a specific power of 105 W/kg [1] under the conditions specified in Table 1. Because of its enhanced performance, the advanced design should exceed the 1983 goal for specific power by a comfortable margin.

Table 3 shows the energies and powers, currents and average cell voltages for ten cells made over about a 3-year period. Values for W h/kg and W/kg were calculated for a six-cell battery module by multiplying the single-cell values for energy and power by 6 and dividing by the module weight, 75 kg. At the 83 A rate, the mean specific energy for the ten cells tested was 45.0 W h/kg. The corresponding volumetric energy density for the module at this rate was 98 W h/l. This compares with 41.5 W h/kg and 88 W h/l for the EV3000 at the same rate. The performance of the advanced cell was very reproducible. The standard deviations for the average cell voltage and power were 0.6% of the mean and for energy, 3.7%, at the 83 A rate.

TABLE 3

Performance of advanced cell design between 20 and 40 cycles

No. of cells tested	Discharge rate (A)	Mean cell voltage (V) (1 σ)	Energy (W h) (1 σ)	Power (W) (1 σ)	Specific energy (W h/kg)	Specific power (W/kg)
1	35.0	1.975	651.5	69.1	52.1	5.53
1	41.5	1.983	635.0	82.2	50.8	6.58
1	65.0	1.950	541.4	126.7	43.3	10.1
10	83.3	1.957 (0.0117)	562.7 (20.88)	163.0 (1.01)	45.0	13.0
2	94.0	1.944	506.9	182.7	40.6	14.6
1	124.5	1.915	485.0	238.5	38.8	19.1

The utilizations of the lead, lead dioxide and sulfuric acid for the EV3000 and advanced cell designs are shown in Table 4 as a percent of theoretical. The utilizations of the positive and negative active materials and the acid are 32%, 11%, and 41% higher, respectively, at the 83 A rate for the advanced design compared with the EV3000. 83 A is the 3-hour rate for the EV3000, whereas the 3-hour rate for the advanced cell is 94 A because its capacity is higher. When the designs are compared at their respective 3-hour rates, the material utilizations of the positive active material and the acid are 19% and 29% higher for the advanced design, but the utilizations of the negative active material are about the same for the two designs.

At all rates the positive active material has the lowest utilization and the acid has the highest utilization. The lower utilization of the positive active material compared with that of the negative is due to the formation of water at the positive electrode, but not at the negative, during discharge. This water dilutes the acid in the pores of the positive plate, causing increased polarization. The 79% acid utilization shown for the advanced cell at 83 A is very close to the maximum practical limit. The discharge capacity is limited almost entirely by the total available acid and the acid concentration is reduced nearly to pure water in the pores of the positive electrode during discharge. However, since the theoretical utilization is based on the acid concentration used in these cells, it may still be possible to increase the energy density by increasing the acid concentration.

TABLE 4

Material utilization of EV3000 and advanced cells

Design	Discharge rate (A)	Theoretical material utilization (%)		
		Positive	Negative	Acid
EV3000	83	31	46	56
Advanced	83	41	51	79
	94	37	46	72

A study of the effect of discharge rate and temperature on the capacities and material utilizations of the negative and positive electrodes used in the advanced cell design was carried out at the currents corresponding to the 3-, 1.5- and 0.75-hour rates and at 23.9, 0, and −17.8 °C. The discharge curves under these various conditions are shown in Figs. 2 and 3 for the positive and negative electrodes, respectively. As expected, the capacity

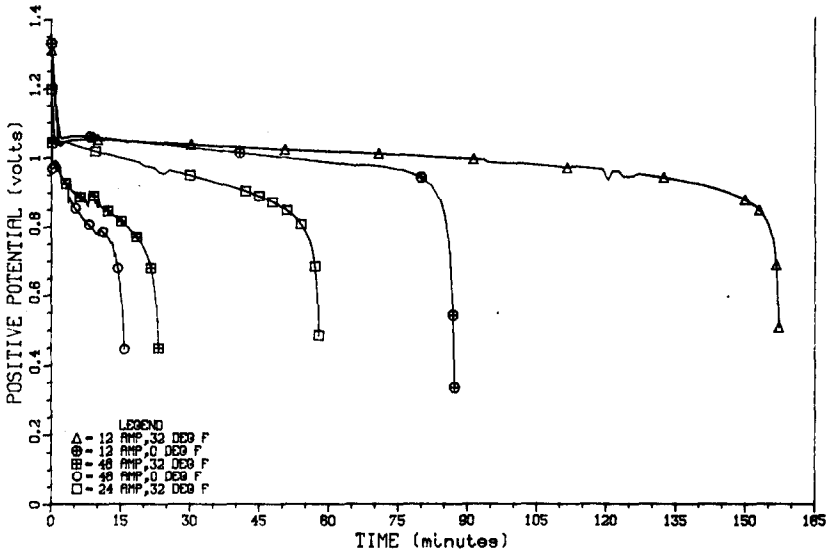

Fig. 2. Positive electrode potential on discharge *versus* $Hg/Hg_2SO_4/5.7\ M\ H_2SO_4$ reference electrode, for different temperatures and discharge rates.

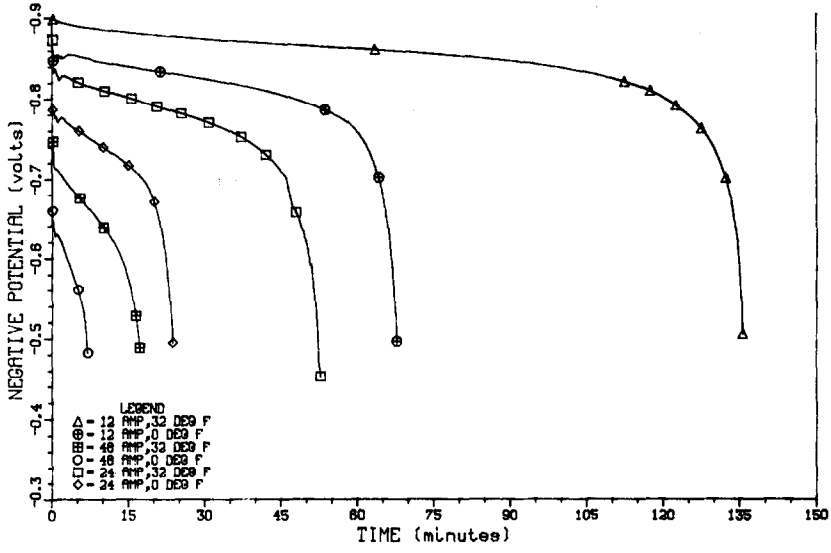

Fig. 3. Negative electrode potential on discharge *versus* $Hg/Hg_2SO_4/5.7\ M\ H_2SO_4$ reference electrode, for different temperatures and discharge rates.

decreases with increasing discharge rate and decreasing temperature for both electrodes.

Peukert plots at the three temperatures are shown in Figs. 4 and 5 for the positive and negative electrodes, respectively. The slope, n, of the Peukert plots for the positive electrode is close to 1.42 and does not vary with temperature. However, for the negative electrode the slope of the

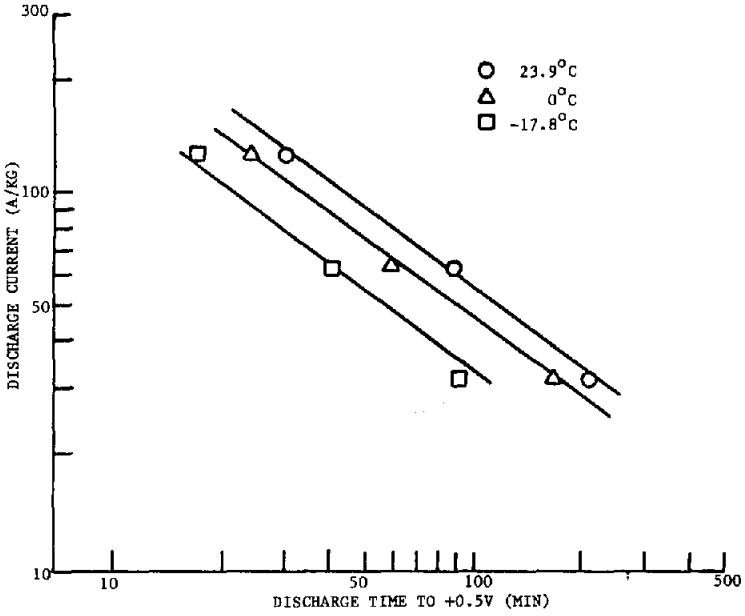

Fig. 4. Peukert plots for positive electrodes at different temperatures.

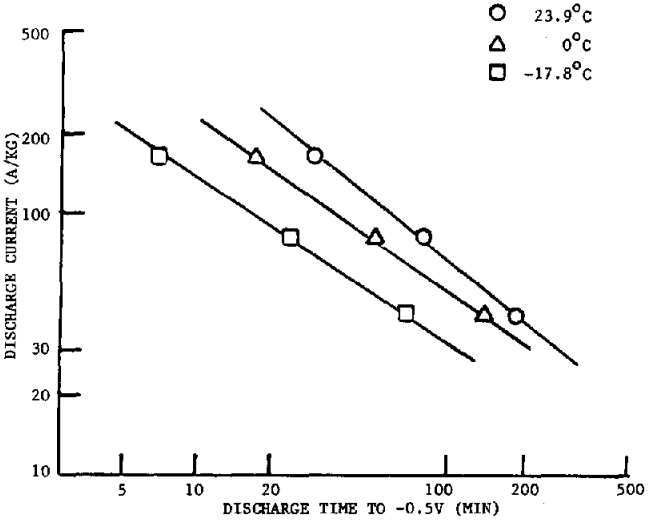

Fig. 5. Peukert plots for negative electrodes at different temperatures.

Peukert plot increases as the temperature increases. The values of n are 1.33, 1.52, and 1.67 for 23.9, 0, and −17.8 °C, respectively.

Tables 5 and 6 show the percentage material utilization of the positive and negative electrodes, respectively, at the various temperatures and discharge rates. The material utilization of both electrodes decreases with decreasing temperature and increasing specific current, but the effect is more severe for the negative electrode. This behavior is characteristic of the lead–acid system. Although the positive electrode limits the capacity of the advanced cell under normal conditions, the negative electrode can become limiting at low temperatures and/or high discharge rates.

Cycle life data for an advanced cell discharged at 83 A to 1.75 V are shown in Fig. 6. Failure was defined as the point where the cell capacity declined to 200 A h. The cell cycled 325 times before reaching this capacity. The mode of failure, which will be discussed in detail in a subsequent paper, appeared to be degradation of the active material in the positive plate. Grid corrosion was not severe. Cycle life tests on EV3000 cells indicated that the cycle life of cells at 80% depth of discharge is more than twice that at 100% depth of discharge when the failure mode is degradation of the positive active material [1]. If the same factor is applied to the advanced design, a cycle life of more that 650 cycles at 80% depth of discharge can be projected.

The energy and coulombic efficiencies of the same cell are shown in Fig. 7 as a function of cycle number. Coulombic efficiencies of 92% - 97% and energy efficiencies of 77% - 84% were achieved. These high efficiencies, which are similar to those of the ISOA designs [1], are due to the acid circulation system.

TABLE 5

Positive active material utilization

Discharge rate per plate	Theoretical material utilization (%) at:		
	23.9 °C	0 °C	−17.8 °C
12 A (3-hour)	53.45	43.71	28.53
24 A (1.5-hour)	49.83	37.10	27.37
48 A (0.75-hour)	43.71	32.86	23.04

TABLE 6

Negative active material utilization

Discharge rate per plate	Theoretical material utilization (%) at:		
	23.9 °C	0 °C	−17.8 °C
12 A (3-hour)	56.43	44.23	23.58
24 A (1.5-hour)	49.65	35.73	18.05
48 A (0.75-hour)	41.18	25.59	11.11

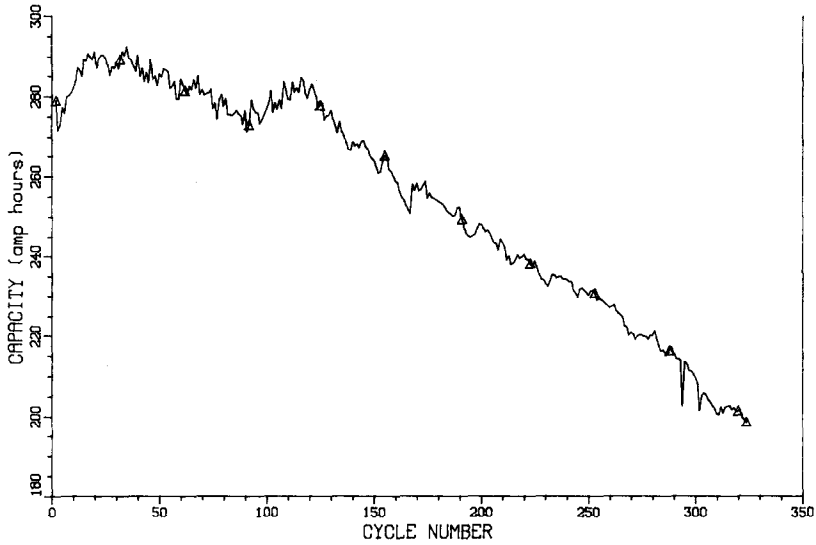

Fig. 6. Capacity of advanced cell cycled using an 83 A discharge rate to 1.75 V (100% depth of discharge).

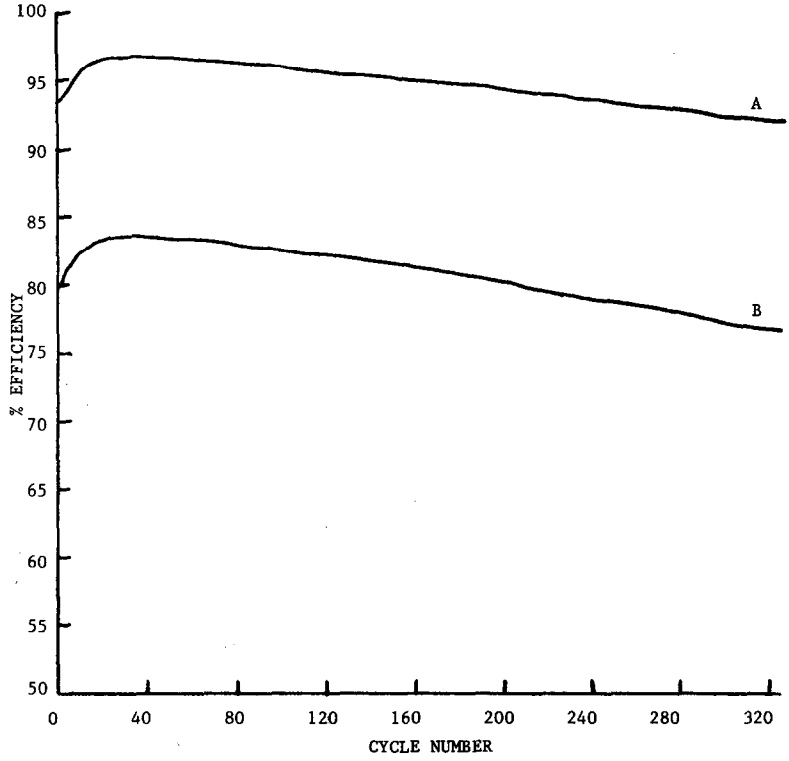

Fig. 7. Coulombic (curve A) and energy (curve B) efficiencies as a function of cycle number for the cell in Fig. 6.

The effect of cell aging on the charging behavior of the advanced cell during 100% depth-of-discharge cycling is shown in Fig. 8. The total cell voltage, current, and half-cell potentials are given for cycles 40, 170 and 250. Table 7 presents the current acceptance as a function of charge voltage at cycles 170 and 270. As the cell ages, the onset of overcharge occurs earlier in the charge period, reflecting a reduction in the time needed to recharge the cell with declining discharge capacity. Although poisoning of the negative electrode by antimony migration has been reported previously [1] with increasing cycle number, it was not noticeable from the negative half-

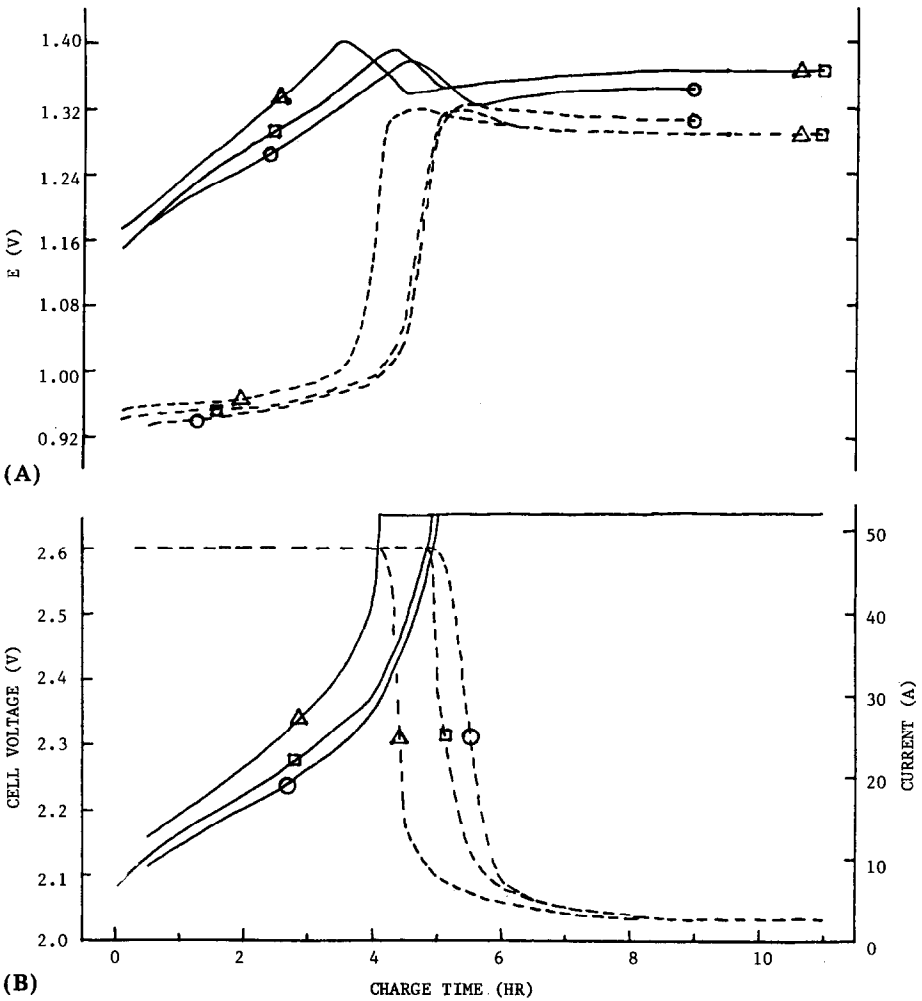

Fig. 8. Charging behavior of an advanced cell for different cycle numbers during 100% depth-of-discharge cycling. A: solid line is positive electrode potential; dashed line is negative electrode potential. B: solid line is cell voltage; dashed line is current. Circles, cycle 40; squares, cycle 170; triangles, cycle 250.

TABLE 7

Current acceptance as a function of charge voltage

Cell voltage	Positive half-cell voltage		Negative half-cell voltage		Current acceptance (steady state) (A)	
	170 cycles	270 cycles	170 cycles	270 cycles	170 cycles	270 cycles
2.65	1.3653	1.3695	−1.2888	−1.2811	2.43	2.52
2.60	1.3460	1.3518	−1.2536	−1.2483	1.29	1.44
2.55	1.3308	1.3373	−1.2193	−1.2124	0.72	0.84
2.50	1.3209	1.3260	−1.1800	−1.1743	0.45	0.54
2.45	1.3168	1.3161	−1.1334	−1.1342	0.27	0.33

cell potential at the end of charge. The current acceptance was nearly constant between 170 and 270 cycles. The cell capacity remained positive limited throughout the cycle test.

Conclusions

The advanced cell design achieved a specific energy of 45 W h/kg and a volumetric energy density of 98 W h/l, compared with 41.5 W h/kg and 88 W h/l for the EV3000 cell, at an 83 A discharge rate. The improvements in specific energy and volumetric energy density compared with those of the EV3000 ISOA battery were achieved by increasing the material utilization of acid and positive active material. Coulombic efficiencies of 92% - 97% and energy efficiencies of 77% - 84% were achieved during the cycle life test. Based on a measured cycle life of 325 cycles in an accelerated test at 100% depth of discharge, a cycle life of over 650 cycles at 80% depth of discharge is projected.

Acknowledgements

The help of our colleagues in Johnson Controls, Inc., Battery Engineering, and in particular of C. E. Weinlein, D. E. Bowman and E. N. Mrotek, is gratefully acknowledged. The leadership and helpful discussions of W. H. Tiedemann are also appreciated. J. L. Strebe and L. Y. Ellzey carried out the cell testing with care and diligence. The Johnson Controls, Inc., Materials Testing Laboratory performed the analyses of failed plate materials.

This work was supported by Johnson Controls, Inc. and by the Department of Energy under the direction of Argonne National Laboratory under Contract No. 31-109-38-4205.

References

1 K. R. Bullock, B. K. Mahato, G. H. Brilmyer and G. L. Wierschem, in K. R. Bullock and D. Pavlov (eds.), *Proc. Symp. on Advances in Lead–Acid Batteries*, The Electrochemical Society, Princeton, NJ, 1984, p. 451.
2 E. N. Mrotek and P. J. Gurlusky, in M. A. Dorgham and J. M. Lafferty (eds.), *Technological Advances in Vehicle Design, Proc. Int. Ass. for Vehicle Design*, Interscience Enterprises, London, U.K., 1982, p. 116.
3 W. Tiedemann and J. Newman, in S. Gross (ed.), *Battery Design and Optimization*, The Electrochemical Society, Princeton, NJ, 1979, pp. 23 - 49.
4 W. Tiedemann and J. Newman, *Summer National Meeting of American Inst. of Chem. Eng., Detroit, MI, 1981*, Paper no. 5378.
5 G. L. Wierschem, *Extended Abstr., Electrochem. Soc. Meeting, Los Angeles, CA, October 1979*, p. 249.
6 B. K. Mahato and W. H. Tiedemann, *J. Electrochem. Soc., 130* (1983) 2139.
7 B. K. Mahato, *J. Electrochem. Soc., 127* (1980) 1679; *128* (1981) 1416.
8 B. Mahato, J. Strebe, D. Wilkinson and K. Bullock, *J. Electrochem. Soc., 132* (1985) 19.
9 M. S. Baxa and C. E. Weinlein, *Extended Abstr., Electrochem. Soc. Meeting, Detroit, MI, October 1982*, p. 11.
10 J. R. Pierson and C. E. Weinlein, in J. Thompson (ed.), *Power Sources 9*, Academic Press, London, U.K., 1983, p. 49.
11 G. L. Wierschem and W. H. Tiedemann, *Extended Abstr., Electrochem. Soc. Meeting, Hollywood, FL, October 1980*, p. 278.
12 D. Thuerk, *Proc. Power Sources Symp., June 1982*, pp. 98 - 91.
13 M. S. Inkmann, *U.S. Pat. 4,221,847* (1980).
14 C. E. Weinlein, *Proc. 9th Energy Technology Conf., Washington, D.C., Feb. 16 - 18, 1982*, pp. 1315 - 1318.
15 D. E. Bowman, *Prog. Batteries Sol. Cells, 5* (1984) 19.
16 B. L. McKinney, G. L. Wierschem and E. N. Mrotek, *SAE Tech. Paper No. 830229*, in *Batteries for Electric Vehicles — Research, Development, Testing and Evaluation*, Int. Autom. Eng. Cong., Detroit, MI, 1983.
17 W. Tiedemann, J. Newman and F. DeSua, in D. H. Collins (ed.), *Power Sources 6*, Academic Press, London, U.K., 1977, p. 15.
18 A. Sabatino and D. Orlando, *U.S. Pat. 3,313,568* (1967) and *3,897,269* (1975).
19 R. M. Fiandt, *U.S. Pat. 3,388,007* (1968).
20 W. Peukert, *Electrotech. Z., 18* (1897) 287.